Defective up-regulation of CD49d in final maturation of NOD mouse macrophages

Sacha Brigitte Geutskens[1,2], Tatjana Nikolic[2], Mireille Dardenne[1], Pieter Johannes Maria Leenen[2] and Wilson Savino[1,3]

[1] CNRS UMR-8147, Necker Hospital, Paris, France
[2] Department of Immunology, Erasmus MC, Rotterdam, The Netherlands
[3] Laboratory on Thymus Research, Department of Immunology, Oswaldo Cruz Institute, Oswaldo Cruz Foundation, Rio de Janeiro, Brazil

Macrophages are potent regulators of both innate and adaptive immunity. They play a central role in the development of autoimmune diabetes and are among the first cells to appear in peri-islet infiltrates of NOD mice that spontaneously develop diabetes. Since efficient adhesion and migration are crucial for proper macrophage trafficking, we examined the migration and fibronectin (FN) adhesion capacity of NOD macrophages, as well as the regulation and expression of the FN receptors $\alpha4\beta1$ and $\alpha5\beta1$. When compared to macrophages from control strains, resident NOD macrophages showed a reduced ability to adhere to and migrate on FN, a delayed clearance following peritoneal inflammation, and substantially lower expression levels of the $\alpha4\beta1$ integrin α chain, CD49d. NOD bone marrow-derived macrophages were specifically defective in the LPS-induced increase in CD49d expression. Moreover, the mitogen-activated protein kinase extracellular signal-regulated kinase-1/2 negatively regulated macrophage CD49d expression and strongly suppressed its expression in NOD macrophages. The data presented herein indicate that the LPS-activated signaling cascade plays a critical role in CD49d expression of macrophages. Mature NOD macrophages are characterized by decreased CD49d expression and show defective CD49d-mediated adhesion to FN.

Received	30/4/04
Revised	20/8/04
Accepted	23/9/04

Key words: NOD / Macrophages / Integrin / Fibronectin / ERK-1/2

1 Introduction

Macrophages form a heterogeneous group of cells, distributed over various tissues. There they form a first line of defense against invading microbial pathogens and regulate both innate and adaptive immune responses. In the NOD mouse, a spontaneous animal model of autoimmune diabetes, macrophages are among the first cells to appear in peri-islet infiltrates, preceding diabetes development [1]. They play an important role in the development of disease, since the selective depletion of macrophages and DC, as well as prevention of their intra-islet infiltration, abrogates diabetes [2, 3].

[DOI 10.1002/eji.200425259]

Abbreviations: BMDM: Bone marrow-derived macrophages **ERK:** Extracellular signal-regulated kinase **FN:** Fibronectin **HRP:** Horseradish peroxidase **MAPK:** Mitogen-activated protein kinase **MCP-1:** Macrophage chemoattractant protein-1 **MEK:** MAPK/ERK kinase **MFI:** Mean fluorescence intensity **pERK:** Phosphorylated ERK **TG:** Thioglycollate **TLR:** Toll-like receptor

Several anomalies have been described for NOD macrophages that might contribute to the development of diabetes. NOD bone marrow-derived macrophages (BMDM) generated *in vitro* fail to mature functionally, and *in vivo*, such a defect may result in a reduced ability to efficiently activate regulatory T cells [4]. Furthermore, NOD BMDM exhibit hyperactivation of the transcription factor NF-κB, leading to elevated expression of IL-12(p70), promoting a Th1-driven immune response [5]. BMDM represent a homogeneous pool of primary macrophages derived from BM precursors. Stimulation of these nonadherent precursors with M-CSF induces an adherent macrophage phenotype, associated with increased expression of the integrin-type fibronectin (FN) receptors $\alpha4\beta1$ and $\alpha5\beta1$ [6].

Integrins form a large family of heterodimeric transmembrane receptors comprised of α and β subunits that specifically recognize extracellular matrix components or cell surface receptors as ligands. The heterodimers $\alpha4\beta1$ (CD49d/CD29) and $\alpha5\beta1$ (CD49e/CD29) recognize the CS-1 and RGD sequence, respectively, of FN, whereas $\alpha4\beta1$ additionally mediates cell-cell adhesion via inter-

© 2004 WILEY-VCH Verlag GmbH & Co. KGaA, Weinheim

action with the addressin VCAM-1 [7, 8]. The regulation of integrin expression and activation is essential for efficient tissue trafficking of macrophages in inflammation. In this context, inflammation of the peritoneal cavity results in the disappearance of resident macrophages [9], and both $\alpha4\beta1$ and $\alpha5\beta1$ are involved in the regulation of macrophage-mesothelial adhesion and transmigration [10]. Regulation of $\alpha4\beta1$ and $\alpha5\beta1$ expression is also essential in the development of diabetes, since inhibition of the interaction of these integrins with their specific ligands prevents diabetes in both induced and spontaneous disease in NOD mice [11, 12].

Different functional aspects of NOD macrophages have been studied with emphasis on the examination of their T cell stimulatory capacity. Efficient adhesion and migration are crucial for proper macrophage trafficking. Since the maturation of NOD macrophages is defective, we reasoned that the expression of the $\alpha4\beta1$ and $\alpha5\beta1$ integrins and related adhesive features might be affected in NOD BMDM. Therefore, we examined CD49d, CD49e and CD49f integrin α chain expression profiles of mature resident macrophages and BM precursors during their differentiation into BMDM in NOD and control mice, in relation to their adhesive capacity. In addition, we studied the mechanisms involved in the regulation of CD49d and CD49e expression related to final macrophage maturation.

2 Results

2.1 Resident NOD macrophages express lower levels of membrane CD49d

We first examined the membrane expression levels of CD49d and CD49e as well as that of the laminin receptor $\alpha6$ chain, CD49f. Peritoneal macrophages were identified by high expression of the macrophage-specific marker BM8 and, like most other peritoneal cells, expressed both CD49d and CD49e (Fig. 1A). By contrast, high levels of CD49f were only expressed by mature peritoneal macrophages (Fig. 1A). Interestingly, unlike blood monocytes (Fig. 1B), mature peritoneal NOD macrophages were characterized by lower CD49d membrane expression levels as compared to macrophages of C57BL/6 and BALB/c strains, independently of the sex (not shown) or age examined (Fig. 1B). No differences in the levels of the $\beta1$ integrin α chains CD49e and CD49f were observed (Fig. 1C). Additionally, $BM8^+$ thymic macrophages of NOD mice showed lower CD49d membrane expression levels as compared to thymic macrophages of control mice (Fig. 1D).

Peritoneal macrophages from male (not shown) or female F1[NOD $\times$ C57BL/6] mice (Fig. 1E) expressed levels of CD49d intermediate to those of macrophages derived from both parental strains. This suggests that the macrophage CD49d membrane expression levels are inherent to the NOD genetic background. Interestingly, peritoneal macrophages of other diabetes-resistant strains like congenic NOD.H-2^b or NOR mice also exhibited higher levels of CD49d as compared to the parental NOD strains (Table 1). By contrast, macrophages of 4-week-old congenic NOD.CD45.1 mice developing diabetes expressed levels of CD49d similar to parental NOD strains (Table 1).

2.2 Resident NOD macrophages show delayed disappearance upon induction of inflammation

Inflammation of the peritoneal cavity results in the disappearance of resident macrophages [9]. This regulated process of macrophage adhesion and mesothelial transmigration depends, at least partly, on the interaction of $\alpha4\beta1$ and $\alpha5\beta1$ [10]. We examined the *in vivo* migratory and adhesive behavior of resident peritoneal macrophages in 3-week-old NOD mice and C57BL/6 mice, in

Table 1. MFI of CD49d in congenic NOD strains

	Strain	MFI CD49d $\pm$ SD	MFI isotype $\pm$ SD	*n* (mice)
A	C57BL/6	360.24$\pm$25.42	2.55$\pm$0.01	6
	NOD	226.94$\pm$9.54	7.48$\pm$3.10	6
	NOD.H-2^b	284.23$\pm$3.86	2.48$\pm$0.14	6
B[a)]	BALB/c	1,342.09$\pm$114.59	31.40$\pm$9.93	3
	NOD	684.81$\pm$29.03	33.00$\pm$11.85	2
	NOR	1,194.59$\pm$190.52	52.53$\pm$18.59	4
C	C57BL/6	311.89$\pm$27.87	4.19$\pm$0.03	6
	NOD	172.83$\pm$1.63	3.97$\pm$0.01	6
	NOD.CD45.1	173.45$\pm$9.00	2.70$\pm$0.16	6

[a)] Analysis was performed on a different flow cytometer.

© 2004 WILEY-VCH Verlag GmbH & Co. KGaA, Weinheim

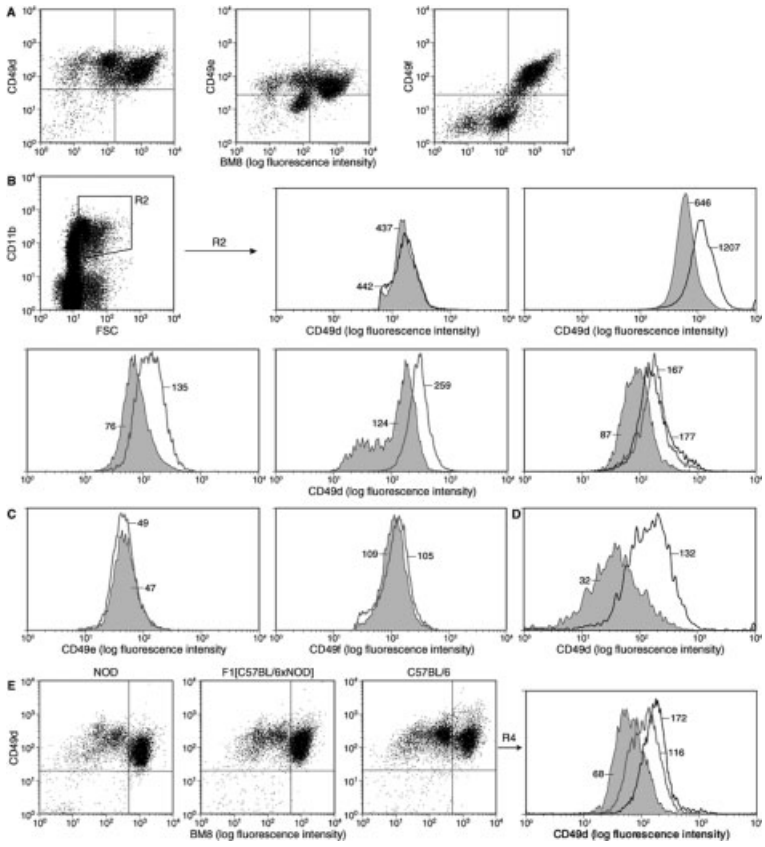

Fig. 1. NOD macrophages exhibit low levels of surface CD49d. (A) Dot plot analysis after cytofluorometry: peritoneal macrophages of 2-week-old C57BL/6 mice stained with BM8 (upper right quadrant) express CD49d (left plot), CD49e (middle) and CD49f (right plot). (B) Upper panels: $FSC^{hi}CD11b^{hi}$ blood monocytes (dot plot, left) were gated, and CD49d levels (middle histogram) of 10-week-old NOD mice (closed graphs) were compared to those of age-matched BALB/c mice (open graphs). Peritoneal $BM8^{hi}$ macrophages of the same mice were also analyzed for CD49d expression (right histogram) using identical settings (NOD, closed graphs; BALB/c, open graphs). Lower panels: histograms show CD49d membrane levels of macrophages of NOD mice (closed graphs) compared to those of C57BL/6 mice (open graphs) at 2 weeks (left) or 14 weeks (middle) of age and compared to C57BL/6 (gray) and BALB/c mice (black) at 4 weeks of age (right). (C) Histograms show CD49e and CD49f levels of peritoneal macrophages of NOD (closed graphs) and C57BL/6 mice (open graphs) at 2 weeks of age. (D) Histogram shows CD49d expression of $BM8^+$ thymic macrophages of NOD (closed graphs) and C57BL/6 (open graphs) mice at 3 weeks of age. (E) Dot plots and histograms show CD49d membrane levels of $BM8^+$ peritoneal macrophages of NOD (closed graph), F1[NOD $\times$ C57BL/6] (grey, open graph) and C57BL/6 (open graph) mice at 2 weeks of age. Experiments were performed with pools of macrophages for young mice and comprised at least five mice per strain and age (n=12 animals per strain). For older mice, cells from individual mice were analyzed. Results are given for one representative experiment selected out of two or more independent experiments. The mean fluorescence intensity (MFI) is depicted for each analysis.

response to inflammation of the peritoneal cavity induced by thioglycollate (TG). For both mouse strains, the frequency of resident $BM8^+$ macrophages decreased in response to TG, 6 and 18 h after TG injection (Fig. 2A). However, total numbers of peritoneal cells increased due to the influx of inflammatory monocytes and granulocytes (not shown). To correct for infiltrating cells, absolute numbers of $BM^{hi}CD49f^+$ resident macrophages were determined, and the percentages of macrophages as compared to the steady state (non-inflamed) situation were calculated. Numbers of resident macrophages decreased by 70% in C57BL/6 mice 6 h after TG injection (Fig. 2B), with a further decrease to 90% after 18 h. In NOD mice, a decrease of only 40% was observed after 6 h as compared to the non-inflamed situation (Fig. 2B), and numbers of resident NOD macrophages hardly decreased thereafter.

2.3 NOD macrophages show a defective interaction with FN

Lower expression of CD49d on $CD34^+$ peripheral blood progenitor cells resulted in decreased adhesion to FN

© 2004 WILEY-VCH Verlag GmbH & Co. KGaA, Weinheim

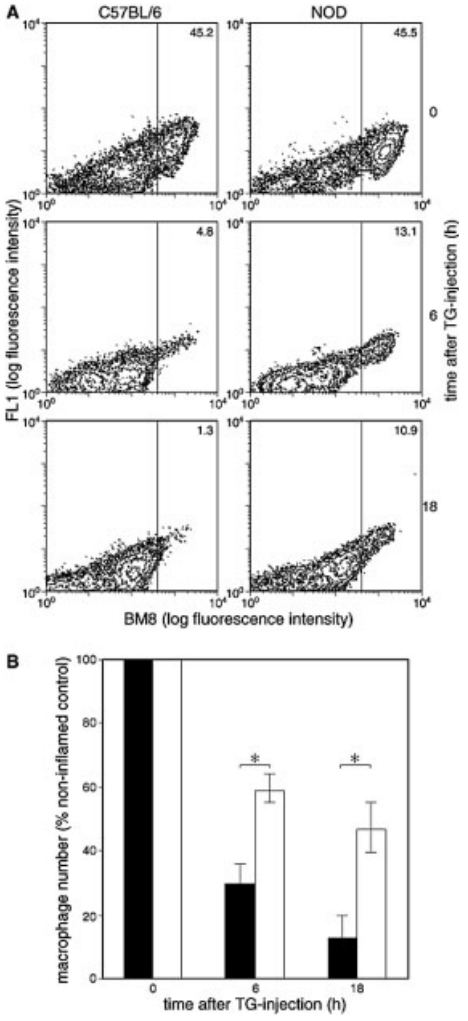

Fig. 2. Resident NOD peritoneal macrophages show delayed disappearance following peritoneal inflammation. (A) Density plots show peritoneal cells stained with BM8 from 3-week-old C57BL/6 or NOD mice before and after TG injection. Frequencies of $BM8^{hi}$ macrophages are depicted. Results are given for one representative experiment selected out of a series of three independent experiments. (B) Percentages of numbers of $BM8^{hi}$ resident macrophages in C57BL/6 (closed bars) and NOD mice (open bars) that remained in the peritoneum after TG injection as compared to the non-inflamed steady state situation, defined as 100% at t=0 h. Data are expressed as the mean of resident macrophages (% non-inflamed control) $\pm$ SEM from mice of two experiments with $^*p<0.05$ (n=6 or more per strain for each given time point).

[13]. Therefore, we examined the capacity of NOD peritoneal macrophages to adhere and migrate to FN.

Resident peritoneal macrophages from both C57BL/6 and NOD mice adhered to FN (Fig. 3A). However, NOD macrophages did so in much lower numbers than C57BL/6-derived peritoneal macrophages, whereas only a minor difference was observed in the $\alpha4\beta1/\alpha5\beta1$-independent adherence to albumin used here as an unrelated protein (Fig. 3A). Similar results were obtained when macrophages were allowed to adhere to the CD49d-specific ligand CS-1 (Fig. 3B), whereas no differences were observed in the adhesion to the CD49e-specific RGD-containing peptide, an unrelated control peptide or albumin (Fig. 3B). When the interaction of $\alpha4\beta1$ with FN was inhibited by the addition of different CD49d-specific blocking antibodies, adhesion to FN was significantly impaired for macrophages of C57BL/6 mice (Fig. 3C). Addition of the CD49d-specific antibodies did not affect the adherence of NOD macrophages to FN (Fig. 3C). These data show that, unlike for C57BL/6 macrophages, CD49d hardly contributed to the adhesion of NOD macrophages to FN.

Furthermore, C57BL/6 macrophages readily migrated through FN-coated filters, as compared to albumin-coated filters, whereas NOD macrophages barely migrated through the FN-coated filters (Fig. 3D). Addition of the chemokine macrophage chemoattractant protein-1 (MCP-1) slightly stimulated the migration of C57BL/6-derived macrophages, but did not rescue the migration of NOD macrophages. Importantly, CD49d-specific antibodies almost completely prevented the MCP-1-stimulated migration of C57BL/6-macrophages, indicating that under these conditions, migration of macrophages on FN is mainly mediated by CD49d.

2.4 NOD-derived BMDM fail to increase CD49d expression following LPS-induced maturation

Membrane density of CD49d and CD49e closely correlates with the stage of macrophage maturation [6]. We examined the integrin expression during the M-CSF-stimulated development of BMDM from BM precursors. No difference was observed in the expression of CD49d, CD49e or CD49f during the development of BMDM when NOD-derived BMDM were compared to BMDM from C57BL/6 or BALB/c mice (not shown).

BMDM are not directly comparable to peritoneal macrophages, since the latter represent a fully differentiated population of cells. In keeping with their developmental stage, peritoneal macrophages were unable to change their integrin profile upon overnight stimulation with LPS or IFN-γ *in vitro* (not shown). We therefore used the homogeneous population of BMDM as a model to examine the expression of CD49d and CD49e upon induction of terminal macrophage development by stimulation with LPS or IFN-γ. Stimulation of BMDM from both C57BL/6 and NOD mice with IFN-γ led to an increase in CD49d membrane expression (Fig. 4A). By

© 2004 WILEY-VCH Verlag GmbH & Co. KGaA, Weinheim

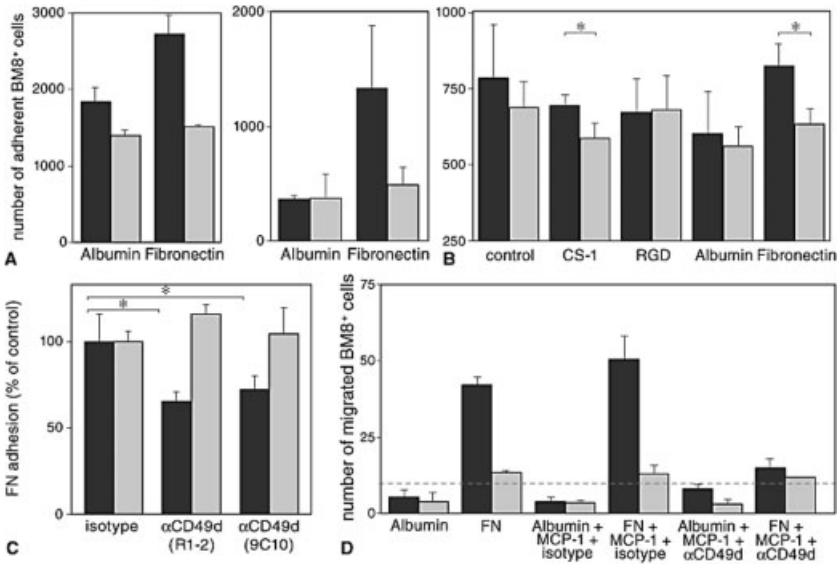

Fig. 3. NOD-derived peritoneal macrophages show defective CD49d-mediated interaction with FN. (A) Graphs show standardized numbers of albumin- or FN-adherent $BM8^+$ C57BL/6 macrophages (black bars) or NOD macrophages (grey bars) at 2 weeks (left) or 14 weeks of age (right). (B) The graph shows standardized numbers of $BM8^{hi}$ C57BL/6 macrophages (black bars) or NOD macrophages (grey bars) adherent to control, CS-1 or RGD peptide, albumin or FN. (C) The graph shows standardized numbers of adherent $BM8^+$ cells from 4-week-old mice after incubation with a CD49d-specific or an unrelated isotype-matched antibody. Adherent cells were counted and related to the number of adherent cells when no antibody was added. (D) The graph shows standardized numbers of $BM8^+$ peritoneal cells of C57BL/6 (black bars) or NOD mice (grey bars) that migrated through FN- or albumin-coated transwell filters, with or without the addition of MCP-1- and CD49d-specific or isotype-matched antibodies. Data are expressed as the mean ± SD, with $^*p<0.05$ of triplicates of one representative experiment (n=5/strain) out of two or more independent experiments.

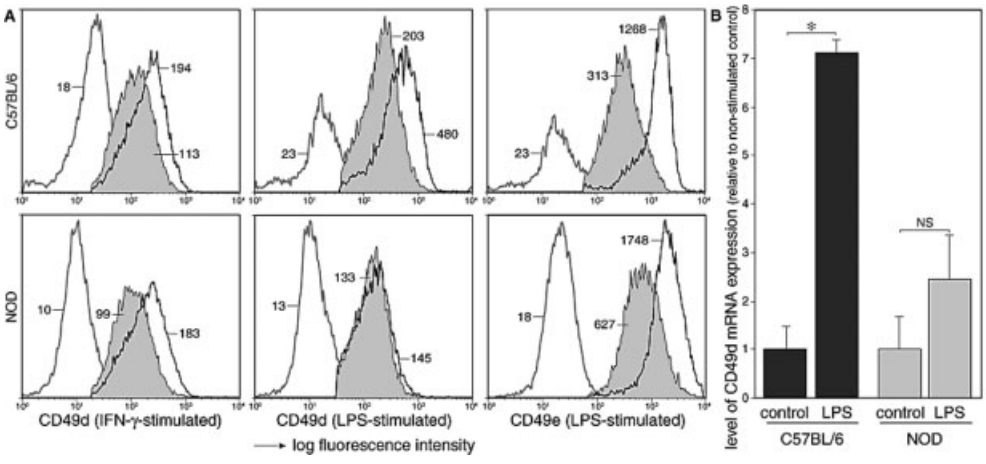

Fig. 4. NOD-derived BMDM fail to enhance CD49d expression upon LPS stimulation. (A) Cytofluorometry profiles of CD49d or CD49e. Grey lines represent isotype-matched controls. The MFI is depicted for each analysis. Left graphs: CD49d levels of C57BL/6-derived BMDM (upper panels) and NOD-derived BMDM (lower panels), not stimulated (closed graphs) and IFN-γ-stimulated (open graphs). Middle graphs: CD49d levels of non-stimulated BMDM (closed graphs) compared to LPS-stimulated BMDM (open graphs). Right graphs: CD49e levels of non-stimulated BMDM (closed graphs) compared to LPS-stimulated BMDM (open graphs). (B) Relative levels of CD49d mRNA expression determined by real-time PCR of LPS-stimulated C57BL/6- (black bars) and NOD-derived (grey bars) BMDM as compared to non-stimulated BMDM, expressed as mean ± SD of triplicates from one representative experiment out of two or more independent experiments. $^*p<0.05$; NS = not significant.

© 2004 WILEY-VCH Verlag GmbH & Co. KGaA, Weinheim

contrast, NOD BMDM failed to increase CD49d expression upon LPS stimulation, unlike BALB/c (not shown) and C57BL/6-derived BMDM (Fig. 4A). Prolongation of the M-CSF cultures for up to 10 days, stimulation with higher concentrations of LPS or prolonged duration of LPS stimulation did not affect the CD49d expression in NOD-derived BMDM (not shown). NOD BMDM did, however, respond to LPS with an increase in the surface expression of CD49e (Fig. 4A) and a decrease in the expression of CD49f (not shown), similar to what was observed for BMDM of the control strains.

To examine whether the increase in integrin surface expression is regulated at the level of gene transcription, we analyzed CD49d and CD49e mRNA expression of non-stimulated or LPS-stimulated BMDM by real-time PCR. CD49e mRNA levels increased upon LPS stimulation in both C57BL/6 and NOD BMDM (not shown). The levels of CD49d mRNA also increased upon LPS stimulation in both strains. However, this increase was twofold higher for C57BL/6 BMDM than for NOD BMDM (Fig. 4B).

2.5 Differential CD49d distribution in BMDM following LPS stimulation

To determine the implications of LPS stimulation, we examined integrin membrane distribution and FN-adhesive properties of LPS-stimulated NOD and C57BL/6 BMDM.

LPS stimulation induced changes in BMDM morphology (Fig. 5A) characterized by swelling of the cell body and formation of more and thinner protrusions. CD49d (Fig. 5A) and CD49e (not shown) molecules relocalized upon LPS stimulation in C57BL/6 BMDM, from a diffuse distribution to a linear staining on the adherent cell edges. This CD49d redistribution was not observed in LPS-stimulated NOD BMDM, although their change in cell morphology was evident (Fig. 5A).

The capacity to adhere to FN increased almost threefold after stimulation with LPS for C57BL/6 BMDM and to a lower extent ($\sim$2.2-fold) for NOD BMDM (Fig. 5B). Interestingly, higher numbers of LPS-stimulated C57BL/6 BMDM adhered to CS-1 peptides and FN as compared to LPS-stimulated NOD BMDM, whereas no differences were observed in the numbers of BMDM adherent to control and RGD peptides or albumin (Fig. 5C). A significant decrease in the numbers of adherent LPS-stimulated C57BL/6 BMDM was observed when the interaction of $\alpha4\beta1$ with FN was inhibited by the addition of CD49d-specific antibodies. By contrast, CD49d-specific antibodies hardly affected the adherence of LPS-stimulated NOD BMDM to FN (Fig. 5D), similar to what was observed for mature peritoneal macrophages. Numbers of FN-adherent LPS-stimulated BMDM from both strains decreased when the interaction of $\alpha5\beta1$ was blocked or when a combination of CD49d- and CD49e-specific antibodies was used (Fig. 5D). Thus, the adhesion to FN was mediated by both $\alpha4\beta1$ and $\alpha5\beta1$ for C57BL/6 BMDM and foremost by $\alpha5\beta1$ for NOD BMDM, confirming earlier observations of mature peritoneal NOD macrophages.

2.6 Inhibition of extracellular signal-regulated kinase-1/2 phosphorylation enhances CD49d expression in both NOD- and C57BL/6-derived BMDM

LPS acts via CD14/Toll-like receptor-4 (TLR-4)-MD2 complexes on the cell surface [14]. The mitogen-activated protein kinase (MAPK) extracellular signal-regulated kinase (ERK)-1/2, downstream of MAPK/ERK kinase (MEK)-1/2, belongs to one of the major signaling pathways that become activated upon TLR-4 stimulation by LPS. We therefore studied the expression of phosphorylated ERK-1/2 (pERK-1/2) in BMDM in response to LPS stimulation.

Day-7 BMDM were analyzed for CD49d and CD49e membrane levels after LPS stimulation, with or without simultaneous incubation with the MEK-1/2 inhibitor UO126. The inhibition of ERK-1/2 phosphorylation, simultaneously with overnight LPS stimulation, enhanced the membrane levels of CD49d in both C57BL/6 and NOD BMDM (Fig. 6A). Levels of CD49d expression did not change when BMDM were incubated with DMSO or UO126 alone (Fig. 6A). Although CD49d membrane levels of NOD BMDM remained lower than that of C57BL/6 BMDM, the magnitude of relative increase in CD49d expression (compared to LPS alone) was similar in both strains.

Immunoblot analysis showed that pERK-1/2 was present in BMDM of both strains as early as 15 min after addition of LPS (Fig. 6B). No pERK-1/2 was detected in non-stimulated cells (Fig. 6B), cells incubated with UO126 alone or BMDM incubated with IFN-γ (not shown). Interestingly, a strong pERK-1/2 signal appeared in LPS-activated NOD BMDM, with earlier kinetics as compared to C57BL/6 BMDM, when equal amounts of protein were loaded (Fig. 6B). Additionally, when related to total ERK protein, the pERK-1/2 signal in LPS-stimulated NOD BMDM also appeared stronger than that of C57BL/6 BMDM (Fig. 6C).

© 2004 WILEY-VCH Verlag GmbH & Co. KGaA, Weinheim

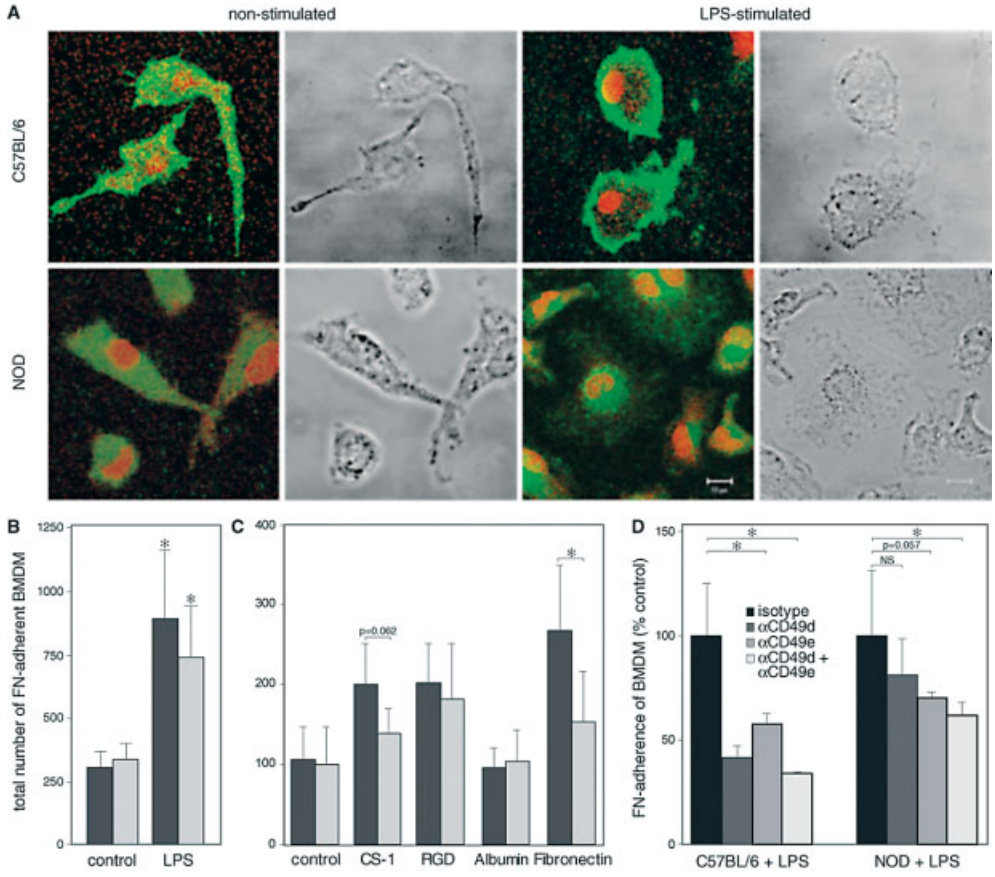

Fig. 5. Differential CD49d distribution in BMDM following LPS stimulation. (A) Confocal microscopy analysis of CD49d expression (green) of adherent day-7 C57BL/6-derived BMDM (upper panel) and NOD-derived BMDM (lower panel), before (left) and after (right) overnight stimulation with LPS. Nuclei are stained with propidium iodide (red). Original magnification: ×1000. (B) The graph shows standardized numbers of non-stimulated or LPS-stimulated day-7 BMDM derived from C57BL/6 (black bars) and NOD (grey bars) mice, adherent to FN. (C) The graph shows standardized numbers of LPS-stimulated day-7 BMDM derived from C57BL/6 (black bars) and NOD (grey bars) mice, adherent to control peptide, CS-1 peptide, RGD peptide, albumin or FN. (D) The graph shows standardized numbers of FN-adherent LPS-stimulated day-7 BMDM from C57BL/6 or NOD mice incubated with specific blocking antibodies prior to FN adhesion. Adherent cells were counted and related to the number of adherent cells when no antibody was added. Data are expressed as the mean ± SD of triplicates from one representative experiment out of two or more independent experiments. *$p<0.05$; NS = not significant.

Furthermore, CD49d mRNA significantly increased in C57BL/6 and NOD BMDM when stimulated with LPS and UO126, as compared to LPS stimulation alone (Fig. 6D). Together, these data show that LPS-induced ERK-1/2 activation negatively regulated macrophage CD49d expression and strongly suppressed the enhancement of CD49d expression of NOD BMDM.

3 Discussion

NOD macrophages display various abnormalities [4, 5]. Here, we show a substantially lower expression level of the $\alpha4\beta1$ integrin α chain CD49d in mature resident NOD macrophages as compared to control strains. Additionally, $\alpha4\beta1$ appeared functionally defective in NOD macrophages, ascertained by their reduced adhesion to and migration on FN and supported by the higher numbers of resident macrophages that remained in the NOD peritoneum upon induction of inflammation, a process previously shown to be partially $\alpha4\beta1$ dependent [10].

The differentiation of BM precursors into BMDM is associated with increased expression levels of $\alpha4\beta1$ and $\alpha5\beta1$ [6]. Here, we show a further increase of CD49d expression levels in BMDM upon induction of final maturation by stimulation with IFN-γ or LPS. Non-stimulated NOD BMDM and peripheral blood monocytes expressed CD49d levels similar to their C57BL/6

© 2004 WILEY-VCH Verlag GmbH & Co. KGaA, Weinheim

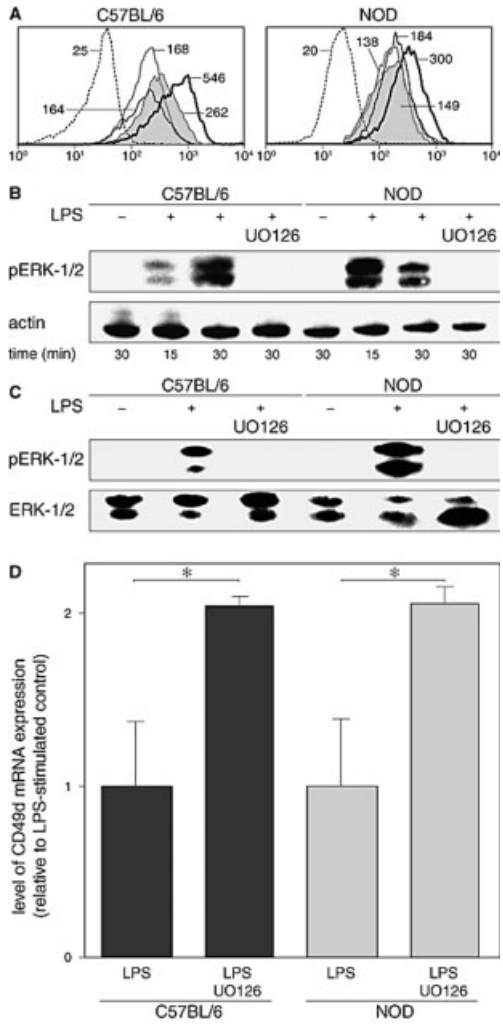

Fig. 6. Inhibition of ERK-1/2 phosphorylation enhances membrane CD49d expression in LPS-stimulated BMDM. (A) CD49d levels of BMDM were determined by cytofluorometry after overnight LPS stimulation (closed graphs) or LPS stimulation and simultaneous inhibition of ERK-1/2 phosphorylation by UO126 (open graphs). Cells incubated with DMSO (grey lines), UO126 (thin black line) or isotype-matched irrelevant mAb (dashed line) served as controls. (B) Immunoblots of BMDM lysates, non-stimulated or stimulated with LPS for different duration with or without UO126, were stained for pERK-1/2 or actin. (C) Immunoblots of BMDM lysates, non-stimulated or stimulated for 15 min with LPS, with or without UO126, were stained for pERK-1/2 or total ERK-1/2. (D) Relative levels of CD49d mRNA expression determined by real-time PCR. Compared to LPS-stimulated BMDM, a twofold increase in the level of CD49d mRNA was observed in both C57BL/6 BMDM and NOD BMDM when the MEK-1 inhibitor UO126 was added. Data are expressed as the CD49d mRNA levels from LPS + UO126-stimulated BMDM over CD49d mRNA levels from LPS-stimulated BMDM; means $\pm$ SD, *$p<0.05$.

counterparts, whereas LPS-matured NOD BMDM were defective in the increase of CD49d expression, like fully developed peritoneal NOD macrophages. This impaired increase in CD49d of NOD BMDM was LPS specific, since stimulation with IFN-γ did increase the levels of CD49d. The defective CD49d increase was not related to a general lack of LPS responsiveness, since NOD BMDM did respond to LPS stimulation with an increase in CD49e mRNA and membrane protein levels, similar to what was observed in control BMDM. In this respect, it is noteworthy that CD49e functionality is regulated differently from that of CD49d, as has been reported earlier [15]. Our data show that both CD49d function, as well as the up-regulation of its expression by LPS, is defective in NOD macrophages, while that of CD49e appears unaffected.

Maturation and increase of CD49d expression in human DC depends on the phosphorylation of p38 MAPK [16], and enhanced maturation of these cells was observed upon inhibition of ERK-1/2 phosphorylation [17]. Although ERK-1/2 and p38 MAPK are both phosphorylated upon LPS stimulation, these signaling molecules usually do not operate in synergy. Moreover, direct "cross-talk" between ERK-1/2 and p38 MAPK resulted in the selective mutual suppression of their activity [18]. High levels of pERK-1/2 were observed early after LPS stimulation in NOD BMDM. Inhibition of ERK-1/2 phosphorylation allowed the increase of CD49d membrane levels and corresponding mRNA expression in both C57BL/6 and NOD BMDM. Interestingly, IFN-γ did up-regulate CD49d in NOD macrophages, and no pERK-1/2 was detected early after stimulation with IFN-γ in BMDM derived from either C57BL/6 or NOD mice (not shown). Hence, LPS-induced ERK-1/2 phosphorylation negatively regulates macrophage CD49d expression and strongly suppresses the increase of CD49d expression in NOD macrophages upon final maturation. The coordinated regulation of the balance between activated MAPK is believed to fine-tune the cellular response to a given stimulus. This balance may be disturbed in NOD macrophages upon stimulation with LPS, leading to high levels of pERK-1/2 and consequent suppression of CD49d expression. Stimulation of NOD macrophages was previously reported to result in hyperactivation of NF-κB [5]. NF-κB might be involved in the regulation of CD49d expression. However, we show that inhibition of ERK-1/2 phosphorylation alone was sufficient to increase CD49d expression in NOD BMDM. The LPS-induced increase in NF-κB binding activity and the increase in the levels of IL-12p40 can be regulated independently of ERK-1/2 activation [19]. Furthermore, NF-κB hyperactivation in NOD macrophages was observed upon activation with various stimuli and was not exclusively restricted to activation with LPS [5]. Thus, NF-κB

© 2004 WILEY-VCH Verlag GmbH & Co. KGaA, Weinheim

hyperactivation in NOD macrophages is probably not involved in the defective CD49d expression following stimulation with LPS.

LPS is a well-studied exogenous activator of TLR-4. Aberrant TLR-4 responsiveness of NOD macrophages may lead to the unbalanced production of cytokines and, as is shown here, plays a critical role in the expression of relevant adhesion molecules like CD49d. Characteristic levels of CD49d and CD49e membrane expression generally reflect phenotypic features of fully differentiated cells, and although the functional properties of $\alpha4\beta1$ and $\alpha5\beta1$ may change upon stimulation, the integrin expression profile usually remains unaffected [20]. Neither LPS nor IFN-γ affected CD49d expression profiles of peritoneal NOD or control macrophages, indicating their fully differentiated phenotype. The encounter of TLR-4 ligands during final macrophage maturation *in vivo* will enhance levels of CD49d in macrophages of control mice. However, activation of the TLR-4 pathway during maturation of NOD macrophages does not lead to enhanced CD49d expression. Fully developed peritoneal and thymic NOD macrophages indeed expressed lower levels of CD49d *in vivo* as compared to various control strains, in accordance with the idea that TLR-4 signaling plays a role in steady state macrophage maturation.

The distinct regulation of $\alpha4\beta1$- and $\alpha5\beta1$-mediated interaction determines their ability to independently mediate migration and adhesion, influenced by the local microenvironment. Low FN concentrations preferentially stimulate the usage of $\alpha5\beta1$ for migration of melanoma cells, whereas $\alpha4\beta1$ usage is favored when FN concentrations increase [15]. Our results show that NOD macrophages are hampered in their CD49d-mediated migratory capacities. Increased numbers of resident macrophages accumulate in the pancreas of neonatal and young NOD mice, even before the onset of insulitis [21]. It would be interesting to examine whether the impaired CD49d-mediated adhesion and migration is involved in the early retention of the macrophages in the pancreas. Such a prolonged local retention may affect the pancreatic microenvironment and favor diabetes development.

Overall, data presented herein show that mature NOD macrophages have decreased CD49d expression and defective CD49d-mediated adhesion to FN. Considering our recent findings showing decreased $\alpha5\beta1$ expression and function in NOD thymocytes [22], it is likely that NOD mice bear multiple FN receptor defects in their distinct hemopoietic lineages.

4 Materials and methods

4.1 Animals

Male and female C57BL/6, BALB/c, NOD, NOD.H-2^b, NOD.CD45.1 and F1[NOD $\times$ C57BL/6] mice, raised in C57BL/6 as well as in NOD female mice, were fed *ad libitum* and bred under specific pathogen-free conditions at Necker Hospital, France, or Erasmus MC, The Netherlands, following the ethical rules provided by the European Union. NOR mice were purchased from Harlan (Horst, The Netherlands). Mice were sacrificed by cervical dislocation.

4.2 Antibodies and reagents

For cytofluorometry, FITC-conjugated anti-Ly6C mAb (own culture) or PE-conjugated mAb against mouse CD49d (clone R1–2 or 9C10), mouse CD49e (clone 5H10–27), or FITC-conjugated anti-human CD49f mAb (clone GoH3) were purchased from PharMingen/Becton Dickinson (Grenoble, France) and were incubated simultaneously with the biotinylated anti-macrophage mAb BM8 (BMA Biomedicals, Augst, Switzerland) or anti-CD11b antibody, detected with streptavidin-PerCP (PharMingen). Purified anti-CD49d, anti-CD49e or isotype control antibodies (PharMingen) were used as blocking antibodies in adhesion assays or as first antibodies for confocal microscopy, followed by incubation with FITC-conjugated goat anti-rat mAb (Jackson Laboratories, West Grove, PA). For immunoblotting, first antibodies specific for ERK-1/2, pERK-1/2 (Sigma Co., St. Quentin Fallavier, France) and actin (Santa-Cruz Biotechnology, Le Perray en-Yvelines, France) were followed by incubation with horseradish peroxidase (HRP)-conjugated swine anti-rabbit or goat anti-mouse antibodies (DAKO, Trappes, France).

Peritoneal macrophages or day-6 BMDM were stimulated for 45 min (real-time PCR) or overnight (FACS analysis) with 10 or 100 ng/ml LPS (*Escherichia coli* strain 055:B5; Sigma Aldrich) or 10 ng/ml murine recombinant IFN-γ (R&D Systems Europe, Lille, France). Phosphorylation of ERK-1/2 was inhibited by the addition of 10 μM MEK-1/2 inhibitor UO126 (Promega France SARL, Charbonnieres, France) 1 h prior to LPS stimulation. The solvent DMSO was used as control.

4.3 Cytofluorometry and confocal microscopy

Peritoneal macrophages were harvested by washing the peritoneal cavity with ice-cold PBS (Invitrogen, Cergy Pontoise, France). Blood monocytes were obtained by heart puncture. Single-cell suspensions of the thymus were prepared by passing the excised thymus through a 100-μm-mesh cell strainer. Cells were counted for individual mice, and adjusted cell numbers of three mice per strain and age were pooled. Cells were directly stained for cytofluoro-

© 2004 WILEY-VCH Verlag GmbH & Co. KGaA, Weinheim

metric analysis, and incubations were performed in 0.1% BSA/PBS. Blood monocytes were identified by their low side scatter and high expression of CD11b, as was described recently [23]. Nonspecific antibody adhesion was blocked by adding anti-FcRγII/III mAb (clone 2.4G2) or 1% normal mouse serum. Samples were analyzed in a FACSCalibur flow cytometer (Becton Dickinson), and results were processed with WinMDI software.

Adherent BMDM grown on glass coverslips (VWR International, Fontenay sous Bois, France) were fixed in 3% formaldehyde for 15 min and washed with PBS. Fixed BMDM were incubated overnight with primary antibodies. Subsequently, slides were washed with PBS-Tween-20 and incubated with appropriate fluorescent secondary antibodies in the presence of 1.5% normal mouse serum. Nuclei were visualized by adding propidium iodide in the last washing step. Coverslips were then embedded in vectashield (Vector laboratories, Burlingame, CA) and examined by confocal microscopy, using the MS 510 Zeiss model device (Germany).

4.4 Immunoblotting

Protein lysates were made after washing adherent BMDM with PBS, removing all PBS by aspiration and adding protein lysate buffer containing 10 mM Tris, 50 mM NaCl, 1% Triton X-100, 30 mM NP_2O_7, 50 mM NaF, 5 μM $ZnCl_2$, 100 μM Na_3VO_4, 1 mM dithiothreitol, 0.5 μM phenylmethylsulfonylfluoride, 5 nM okadaic acid, 0.5 mM benzamidine and EDTA-free protease inhibitor cocktail (Complete mini; Roche, Mannheim, Germany). The protein contents of the lysates were determined in duplicate with the bicinchoninic acid protein assay (Pierce, Rockford, IL). Of lysates, 10 μg were resolved in 4–12% gradient Precast Nupage Bis-Tris gels (Invitrogen, Paisley, UK) in standard Laemmli's loading buffer (100 mM Tris, 4% SDS, 30% glycerol and 2-mercaptoethanol) containing 0.2 M dithiothreitol and transferred using semi-dry blotting onto Hybond C-extra nitrocellulose membranes (Amersham, Buckinghamshire, UK). Blots were washed with Tris-buffered saline and stained with Ponceau Red to control for the blotting efficiency. Nonspecific binding sites were blocked with Tris-buffered saline containing 5% powder milk, followed by incubation with first antibodies. Blots were washed and incubated with the appropriate HRP-conjugated secondary Abs. HRP activity was visualized using the supersignal kit with ECL hyperfilms (Amersham). Colored kaleidoscope broad-range markers (Bio-Rad, Ivry, France) were used to indicate protein size. The chemiluminescence signal was detected with Kodak films or counted directly by an electronically cooled LAS-1000 plus charge-coupled device camera system and analyzed with Image Gauche 4.0 software (Fuji Photo Film Co., Tokyo, Japan).

4.5 Real-time PCR

Total RNA was extracted from adherent BMDM using RNAble reagent (Eurobio, Les Ulis, France), according to the manufacturer's instructions. RNA concentrations were measured by optical absorbance at 260 nm, and the samples were subsequently stored at –80°C. Total RNA (2 μg) was reverse transcribed using a reverse transcription system (Promega) according to the manufacturer's instructions, in the presence of Oligo dT15 and random hexamers. Partial cDNA for CD49d or CD49e integrin α chains were amplified by using specific primer pairs (CD49d forward: 5′ GAATCCAAACCAGACCTGCGA 3′; CD49d reverse: 5′ TGACGTAGCAAATGCCAGTGG 3′; CD49e forward: 5′ CTGTGATTTTCCCAGTCAGCC 3′; CD49e reverse: 5′ TGCAGTTGCTGAGTCCTGTCA 3′) by real-time PCR using Sybergreen reagent (Eurogentec, Herstal, Belgium) and β2-microglobulin or β-actin as internal references. Amplification was measured with the ABI Prism 7700 Sequence Detection System and analyzed with ABI Prism Sequence Detector v1.6.3 software (Applied Biosystems, Courtaboeuf, France).

4.6 *In vivo* macrophage disappearance response

Three-week-old mice weighing 10–15 g were injected i.p. with 50 μl/g 3% TG broth (Biomerieux, Marcy-Etoile, France). Peritoneal macrophages were harvested 6 or 18 h after injection and stained as described above. Cells were kept on ice during the entire procedure. The experiment was repeated three times comprising a total of six to twelve mice per strain/group.

4.7 Macrophage adhesion and transmigration assays

Flat-bottom culture plates (96-well) or transwell filters (8 μm pore size; Corning Costar Corporation, Cambridge, MA) were coated overnight at 4°C with 10 μg/ml albumin (Sigma-Aldrich), FN (Chemicon International, Temecula, CA) or CD49d- or CD49e-specific FN ligands [CS-1 peptide, RGD peptide or an inactive analog (GRGESP); BACHEM Biochimie SARL, Voisins-le-Bretonneux, France]. Wells or filters were washed three times with sterile PBS, and nonspecific sites were blocked with 1% BSA for 1 h at 37°C. Wells were washed twice with PBS and once with RPM1 1640-glutamax completed with 0.5% FCS (Invitrogen, Cergy Pontoise, France). Freshly harvested peritoneal macrophages or day-7 BMDM were added at a concentration of 5×10^4/ml in 100 μl RPMI-0.5% FCS and incubated for 30 min at 37°C. To standardize macrophage numbers, the percentage of $BM8^{hi}$ macrophages was determined in parallel using cytofluorometry. After 30 min of adhesion, nonadherent cells were removed by gentle aspiration and washing with RPMI medium. Adherent cells were fixed and stained with the RAL-555 fast-staining kit (RAL REACTIFS, Bordeaux,

© 2004 WILEY-VCH Verlag GmbH & Co. KGaA, Weinheim

France). For migration assays, 2×10^4/ml peritoneal cells were added in 100 μl RPMI-0.5% FCS to the upper compartment and incubated for 4 h at 37°C to allow migration to the lower compartment filled with 600 μl RPMI-0.5% FCS, with or without 100 ng/ml MCP-1 (Peprotech, Rocky Hill, NJ). Migrated cells were stained with BM8 to determine the absolute number of migrated macrophages. When blocking antibodies were applied, adjusted macrophage numbers were incubated for 30 min on ice with 1 mg/ml of antibody prior to adhesion. Each condition was tested in triplicate in two or three independent experiments.

4.8 Culture of BMDM with M-CSF

Mice (2 or 4 weeks old) were sacrificed by cervical dislocation. Their femurs and tibiae were collected, and muscle tissue was removed. BM single-cell suspensions were prepared as described [24], and cells were seeded in sterile culture dishes (Falcon) at 4×10^6 cells/10 ml in RPMI 1640-glutamax enriched with 10% FCS and 50 ng/ml recombinant murine M-CSF (R&D Systems, Abingdon, UK). Cultures were maintained for 7 days without refreshing culture media.

4.9 Statistical analysis

Data of disappearance and adhesion assays, as well as data of real-time PCR, were expressed as mean ± SD or SEM; *p*-values were calculated with the two-tailed Student's *t*-test for unpaired values.

Acknowledgements: We are grateful to Drs. A. Hans, G. Milon and M. Leite-de-Moraes for providing reagents, Dr. R. Milner, Dr. F. Lepault and Mrs. M. C. Gagnerault for helpful advice, and Drs. D. V. Serreze, J. J. Bajramovic, F. Homo-Delarche and H. A. Drexhage for critically reading this manuscript. This work was supported by the Centre Nationale de la Recherche Scientifique and grants from the European committee (QLRT-1999–00276-"MONO-DIAB").

References

1 **Jansen, A., Homo-Delarche, F., Hooijkaas, H., Leenen, P. J. M., Dardenne, M. and Drexhage, H. A.,** Immunohistochemical characterization of monocytes-macrophages and dendritic cells involved in the initiation of the insulitis and beta-cell destruction in NOD mice. *Diabetes* 1994. **43:** 667–675.

2 **Hutchings, P., Rosen, H., O'Reilly, L., Simpson, E., Gordon, S. and Cooke, A.,** Transfer of diabetes in mice prevented by blockade of adhesion-promoting receptor on macrophages. *Nature* 1990. **348:** 639–642.

3 **Jun, H. S., Yoon, C. S., Zbytnuik, L., van Rooijen, N. and Yoon, J. W.,** The role of macrophages in T cell-mediated autoimmune diabetes in nonobese diabetic mice. *J. Exp. Med.* 1999. **189:** 347–358.

4 **Serreze, D. V., Gaedeke, J. W. and Leiter, E. H.,** Hematopoietic stem-cell defects underlying abnormal macrophage development and maturation in NOD/Lt mice: defective regulation of cytokine receptors and protein kinase C. *Proc. Natl. Acad. Sci. USA* 1993. **90:** 9625–9629.

5 **Sen, P., Bhattacharyya, S., Wallet, M., Wong, C. P., Poligone, B., Sen, M., Baldwin Jr., A. S. and Tisch, R.,** NF-kappa B hyperactivation has differential effects on the APC function of nonobese diabetic mouse macrophages. *J. Immunol.* 2003. **170:** 1770–1780.

6 **Shima, M., Teitelbaum, S. L., Holers, V. M., Ruzicka, C., Osmack, P. and Ross, F. P.,** Macrophage-colony-stimulating factor regulates expression of the integrins alpha 4 beta 1 and alpha 5 beta 1 by murine bone marrow macrophages. *Proc. Natl. Acad. Sci. USA* 1995. **92:** 5179–5183.

7 **Takada, Y., Huang, C. and Hemler, M. E.,** Fibronectin receptor structures in the VLA family of heterodimers. *Nature* 1987. **26:** 607–609.

8 **Elices, M. J., Osborn, L., Takada, Y., Crouse, C., Luhowskyj, S., Hemler, M. E. and Lobb, R. R.,** VCAM-1 on activated endothelium interacts with the leukocyte integrin α4β1 at a site distinct from the α4β1/fibronectin binding site. *Cell* 1990. **60:** 577–584.

9 **Melnicoff, M. J., Horan, P. K. and Morahan, P. S.,** Kinetics of changes in peritoneal cell populations following acute inflammation. *Cell. Immunol.* 1989. **118:** 178–191.

10 **Bellingan, G. J., Xu, P., Cooksley, H., Cauldwell, H., Shock, A., Bottoms, S., Haslett, C., Mutsaers, S. E. and Laurent, G. J.,** Adhesion molecule-dependent mechanisms regulate the rate of macrophage clearance during the resolution of peritoneal inflammation. *J. Exp. Med.* 2002. **196:** 1515–1521.

11 **Yang, X. D., Michie, S. A., Tisch, R., Karin, N., Steinman, L. and McDevitt, H. O.,** A predominant role of integrin alpha 4 in the spontaneous development of autoimmune diabetes in nonobese diabetic mice. *Proc. Natl. Acad. Sci. USA* 1994. **91:** 12604–12608.

12 **Burkly, L. C., Jakubowski, A. and Hattori, M.,** Protection against adoptive transfer of autoimmune diabetes mediated through very late antigen-4 integrin. *Diabetes* 1994. **43:** 529–534.

13 **Prosper, F., Stroncek, D., McCarthy, J. B. and Verfaillie, C. M.,** Mobilization and homing of peripheral blood progenitors is related to reversible downregulation of alpha4 beta1 integrin expression and function. *J. Clin. Invest.* 1998. **101:** 2456–2467.

14 **Takeuchi, O., Hoshino, K., Kawai, T., Sanjo, H., Takada, H., Ogawa, T., Takeda, K. and Akira, S.,** Differential roles of TLR2 and TLR4 in recognition of gram-negative and gram-positive bacterial cell wall components. *Immunity* 1999. **11:** 443–451.

15 **Hangan-Steinman D., Ho. W. C., Shenoy. P., Chan. B. M. and Morris. V. L.,** Differences in phosphatase modulation of alpha4beta1 and alpha5beta1 integrin-mediated adhesion and migration of B16F1 cells. *Biochem. Cell Biol.* 1999. **77:** 409–20.

16 **Puig-Kroger, A., Sanz-Rodriguez, F., Longo, N., Sanchez-Mateos, P., Botella, L., Teixido, J., Bernabeu, C. and Corbi, A. L.,** Maturation-dependent expression and function of the CD49d integrin on monocyte-derived human dendritic cells. *J. Immunol.* 2000. **165:** 4338–4345.

17 **Puig-Kroger, A., Relloso, M., Fernandez-Capetillo, O., Zubiaga, A., Silva, A., Bernabeu, C. and Corbi, A. L.,** Extracellular signal-regulated protein kinase signaling pathway negatively regulates the phenotypic and functional maturation of monocyte-derived human dendritic cells. *Blood* 2001. **98:** 2175–2182.

18 **Hall, J. P. and Davis, R. J.,** Inhibition of the p38 pathway upregulates macrophage JNK and ERK activities, and the ERK, JNK, and p38 MAP kinase pathways are reprogrammed during

© 2004 WILEY-VCH Verlag GmbH & Co. KGaA, Weinheim

differentiation of the murine myeloid M1 cell line. *J. Cell. Biochem.* 2002. **86:** 1–11.

19 **Zhang, J., Feng, W., Li, C., Wang, X. and Chang, Z.,** NF-kB regulates LPS-induced expression of interleukin 12 p40 in murine peritoneal macrophages: roles of PKC, PKA, ERK, p38 MAPK, and proteosome. *Cell. Immunol.* 2000. **204:** 38–45.

20 **Chan, B. M., Wong, J. G., Rao, A. and Hemler, M. E.,** T cell receptor-dependent, antigen-specific stimulation of a murine T cell clone induces a transient, VLA protein-mediated binding to extracellular matrix. *J. Immunol.* 1991. **147:** 398–404.

21 **Charré, S., Rosmalen, J. G., Pelegri, C., Alves, V., Leenen, P. J. M., Drexhage, H. A. and Homo-Delarche, F.,** Abnormalities in dendritic cell and macrophage accumulation in the pancreas of nonobese diabetic (NOD) mice during the early neonatal period. *Histol. Histopathol.* 2002. **17:** 393–401.

22 **Cotta-de-Almeida, V., Villa-Verde, D. M. S., Lepault, F., Pleau, J. M., Dardenne, M. and Savino, W.,** Impaired migration of NOD thymocytes: a fibronectin receptor-receptor defect. *Eur. J. Immunol.* 2004. **34:** 1578–1587.

23 **Sunderkotter, C., Nikolic, T., Dillon, M. J., Van Rooijen, N., Stehling, M., Drevets, D. A. and Leenen, P. J.,** Subpopulations of mouse blood monocytes differ in maturation stage and inflammatory response. *J. Immunol.* 2004. **172:** 4410–4417.

24 **de Bruijn, M. F., Slieker, W. A., van der Loo, J. C., Voerman, J. S., van Ewijk, W. and Leenen, P. J. M.,** Distinct mouse bone marrow macrophage precursors identified by differential expression of ER-MP12 and ER-MP20 antigens. *Eur. J. Immunol.* 1994. **24:** 2279–2284.

Correspondence: Sacha Brigitte Geutskens, Department of Immunology, Erasmus MC, Dr. Molewaterplein 50, PO Box 1738, 3000 DR Rotterdam, The Netherlands
Fax: +31-10-408-9456
e-mail: s.geutskens@erasmusmc.nl

© 2004 WILEY-VCH Verlag GmbH & Co. KGaA, Weinheim